

Aging Differences of Colored Microplastics and Their Adsorption Behavior towards Acesulfame

Xiuli Li¹, Fangyu Bin¹, Zhenzhen Zhou¹, Jin Cui¹, Hongyu Shan^{1,*}

¹School of Life and Environmental Science, Guilin University of Electronic Technology, Guilin, Guangxi, 541000, China

*Corresponding author

Abstract: This study investigated the aging behavior differences of MPs of different colors under UV light aging and thermal activation of $K_2S_2O_8$ chemical oxidation, as well as their adsorption characteristics towards the artificial sweetener acesulfame. By simulating photoaging and chemical oxidation in the laboratory, and combining surface morphology, chemical structure, and adsorption kinetics/isotherm models, the impact of color on the aging process and the adsorption behavior of aged MPs were systematically assessed. The results showed that the aging effect of thermal activation of $K_2S_2O_8$ was significantly better than that of UV light aging, with the CI of red PE increasing the most (photoaging: 0.0765; chemical oxidation: 0.1081), and the surface wrinkles and cracks increased, providing more adsorption sites. Color had a significant impact on photoaging, with red PE aging and fading more easily due to its light absorption characteristics, while black MPs had a lower degree of aging due to the shading effect and the action of antioxidants. Aging significantly enhanced the adsorption capacity of PE for acesulfame, with the highest adsorption amount of PE treated by thermal activation of $K_2S_2O_8$ (2.478 mg/g), which was 33.8% higher than that of the original PE. Adsorption kinetics indicated that the adsorption process of the original and photoaged PE conformed to the pseudo-first-order model (dominated by physical adsorption), while the PE treated by chemical oxidation conformed more to the pseudo-second-order model (synergistic effect of physical and chemical actions). Isotherm adsorption followed the Freundlich model, indicating a multilayer heterogeneous adsorption mechanism. This study revealed the regulatory effect of color on the aging behavior of MPs and clarified the mechanism by which the aging process enhanced the adsorption capacity for pollutants by changing surface physicochemical properties. It provides a theoretical basis for assessing the environmental risk of colored MPs and the migration and transformation of artificial sweeteners.

Keywords: Colored microplastics; UV aging; Thermal activation of $K_2S_2O_8$ aging; Acesulfame; Adsorption

1. Introduction

Due to the widespread dependence on plastic products and their aging behavior in the environment, the generation and environmental behavior of microplastics (MPs) have increasingly attracted attention. The color of plastic products is intentionally produced based on their actual use, playing a special role in product aesthetics, management operations, safety warnings, and drug identification [1]. Therefore, colored MPs in the natural environment also have a high abundance. The difference in color is the most obvious physicochemical property difference that people can directly observe in the same type of MPs. Due to the difference in the light absorption of the color itself and the characteristics of the additives used to form the color, the environmental behavior of MPs of different colors may have significant differences [2, 3]. However, previous studies on MPs often used white or transparent samples for discussion, or used commercial plastic products without specifically mentioning the color for exploration, thus ignoring the potential impact of the color of MPs.

The aging behavior of MPs significantly changes their physicochemical properties. Therefore, the assessment of the environmental behavior of MPs inevitably considers the differences before and after aging [4]. However, there are opposite views on the impact of color on the aging of MPs. Zhao et al. [1] pointed out that MPs of long-wavelength colors have a weaker shading effect than those of short-wavelength colors, so they age more slowly. However, Li et al. [4] pointed out that MPs of long-wavelength colors are more prone to aging than those of short-wavelength colors. Therefore, the impact of plastic color on the aging of MPs needs further discussion.

The aging behavior of MPs is closely related to the aging method^[5, 6]. Given the long half-life of MPs in the environment^[7], laboratory accelerated aging simulation experiments are an important means to explore the aging process of MPs in the natural environment^[8]. Among them, photoaging and chemical oxidation are the two most common methods^[9, 10]. Photoaging is mainly affected by the light absorption of the plastic color itself and the additives in the plastic. In contrast, chemical oxidation mainly occurs through chemical reactions between oxidants (such as persulfate, ozone, etc.) and plastic molecules, and the process is not affected by the light absorption of the plastic color itself. Therefore, MPs of different colors may show significant differences in the processes of photoaging and chemical oxidation^[2, 5]. In summary, exploring the impact of photoaging and chemical oxidation on the aging of MPs of different colors not only helps to deepen the understanding of the potential regulation of plastic color on the aging of MPs but also provides an important theoretical basis for assessing the environmental behavior and ecological risk of colored MPs.

Artificial sweeteners have become a research focus due to their environmental persistence and potential ecological toxicity^[11]. Although there is currently no conclusive evidence of direct harm to humans from artificial sweeteners, their accumulation in the environment is continuously increasing, and their environmental risks still need further investigation^[12]. In the environmental system, MPs, with their large specific surface area and strong adsorption capacity, are prone to adsorption with artificial sweeteners^[11]. It is worth noting that MPs can cause synergistic toxicity through the carrier effect, thereby further exacerbating the biological toxicity of low-risk pollutants entering the human body^[13]. Therefore, exploring the adsorption of MPs for artificial sweeteners helps to further assess the environmental risks and ecological impacts of these two types of new pollutants.

In this study, four common colors (black, white, red, and blue) of polyethylene (PE) commercial plastic bags were manually prepared into corresponding colored MPs. In the laboratory, UV irradiation photoaging and thermal activation of persulfate ($K_2S_2O_8$) chemical oxidation experiments were carried out, and the adsorption behavior of MPs for acesulfame before and after aging was monitored. The aims of this study were to (1) analyze the potential regulatory effect of color on the aging of MPs by comparing the aging differences of MPs of different colors under the two aging methods; (2) explore the adsorption behavior of MPs for acesulfame before and after aging. The conclusions were drawn through field emission scanning electron microscopy (FESEM), attenuated total reflectance Fourier transform infrared spectroscopy (ATR-FTIR), and the fitting analysis of adsorption kinetics and isotherm models. This study emphasized the potential regulation of plastic color on the aging behavior of MPs and also examined the possibility of MPs providing a carrier for artificial sweeteners. It provides a research basis for a deeper understanding of the ecological risks of MPs.

2. Materials and Methods

2.1. Experimental Materials

In this study, four colors of commercial PE plastic bags were purchased from Qiaoyang Packaging Factory, Ningjin County, Xingtai City, Hebei Province, China. The plastic bags were punched into particles with a diameter of 1 mm using a hole puncher. Subsequently, the particles were washed three times with anhydrous ethanol to remove surface organic matter, followed by three washes with ultrapure water. The samples were then filtered through qualitative filter paper and dried at 40°C. After processing, the samples were stored in the dark at room temperature for subsequent use. Other chemicals used in the experiment, such as potassium persulfate and acesulfame, were purchased from Aladdin Reagents (Shanghai) Co., Ltd.

2.2. Laboratory Simulated Accelerated Aging of MPs

2.2.1. Photoaging

A self-made photoaging reaction chamber was used to conduct a 16-day accelerated UV aging simulation experiment on PE samples of different colors. The main body of the reaction chamber was made of stainless steel, equipped with a 250W mercury lamp (Philips TL-K40W10R) at the top, with a spectral range of 254-700 nm and a peak wavelength of 365 nm. A radiometer (SM206-SOLAR, Xinbao Technology Co., Ltd., Shanghai, China) was used to monitor the UV irradiance of the light source at 5 mW/cm². During the photoaging process, the laboratory temperature was maintained at 22°C, and the humidity was controlled at 65%. Two 20W adjustable power exhaust fans were installed on each side of the reaction chamber to control the internal temperature of the chamber at 25±2°C.

2.0 g of PE samples were placed in a 10 cm diameter open petri dish directly below the mercury lamp for photoaging. A quartz cover was placed on the surface of the petri dish to minimize unnecessary interference. The petri dish was manually shaken every 8 hours to ensure that all surfaces of the PE samples were evenly exposed to UV light. The light irradiance received on the surface of the samples was monitored at 2 mW/cm².

2.2.2. Thermal Activation of K₂S₂O₈ Aging

According to the experimental method of Liu et al. [14], 2 g of PE samples were added to 20 mL of K₂S₂O₈ solution (100 mM), and the pH was adjusted to 7.0. The mixture was placed in a constant temperature water bath with stirring function, and the temperature was set at 70°C to maintain the optimal activation efficiency of K₂S₂O₈. Due to the consumption of K₂S₂O₈ during the aging process, an equal amount of K₂S₂O₈ solution was added every 12 hours. Every 2 days, the PE samples were filtered and separated, washed three times with deionized water, and then mixed with fresh K₂S₂O₈ solution to avoid the accumulation of K₂S₂O₈. After 16 days of continuous aging treatment, the PE samples were separated, washed and filtered three times with deionized water, dried in a 40°C oven, and stored in brown glass bottles.

2.2.3. Characterization of Aged PE Samples

The surface morphological characteristics of PE samples of different colors before and after aging were analyzed using a field emission scanning electron microscope (Quanta 450 FEG, FEI, USA). The chemical composition and molecular structure information on the surface of PE samples were obtained using an attenuated total reflectance Fourier transform infrared spectrometer (Nicolet IS20, Thermo Scientific, USA). The carbonyl index (CI) was used to quantitatively determine the degree of aging of PE samples, and the calculation formula is as follows:

$$CI = \frac{A_{C=O}}{A_{C-H}}$$

where $A_{C=O}$ represents the absorption peak area of the C=O characteristic peak in the range of 1900-1650 cm⁻¹, and A_{C-H} represents the absorption peak area of the C-H characteristic peak in the range of 2960-2850 cm⁻¹.

2.3. Adsorption Experiments of MPs for Acesulfame

In the adsorption experiment, 50 mg of original, 16-day photoaged, and 16-day thermally activated K₂S₂O₈-aged red PE samples were respectively weighed and placed in 100 mL conical flasks, and mixed with 50 mL of acesulfame solution with different initial concentrations. The conical flasks were placed in a constant temperature shaking incubator at 25°C and 180 r/min. For the adsorption kinetics experiment, a acesulfame solution with a concentration of 5 mg/L was used, and the sampling times were set at 0, 1, 2, 4, 8, 12, 24, and 48 hours. For the adsorption isotherm experiment, acesulfame reaction solutions with concentrations of 1, 3, 5, 8, and 10 mg/L were used, and the sampling times were set at 0, 2, 4, 8, 12, and 24 hours. The collected solutions were all filtered through a 0.22 μm polyethersulfone (PES) filter membrane, and the residual concentration of acesulfame solution was quantified using a high-performance liquid chromatograph (U3000, Thermo Scientific, USA).

The quantification of high-performance liquid chromatography was carried out using the external standard method, and the test conditions were as follows: a C18 reverse-phase chromatography column was used, the mobile phase was composed of methanol and 0.02 mol/L ammonium acetate aqueous solution, isocratic elution mode was adopted, methanol: ammonium acetate aqueous solution = 10:90% (v:v), the flow rate was 1 mL/min, and the detection wavelength was 230 nm.

3. Results and Discussion

3.1. Changes in Properties of Different Colored PE before and after Aging

3.1.1. Surface Morphology Changes

As shown in **Figure 1**, the surfaces of the original PE of different colors were relatively smooth, with no obvious wrinkles or protrusions. However, after being treated with the two different aging methods, the surfaces of the MPs exhibited significant wrinkles and cracks, and their shapes became irregular. These changes may have provided more potential adsorption sites for the MPs, thereby potentially

enhancing their adsorption capacity [15]. The aging effects of the two methods on the MPs were both significant, and no obvious differences were observed at different scales, indicating the need for further quantitative analysis of the aging degree of PE.

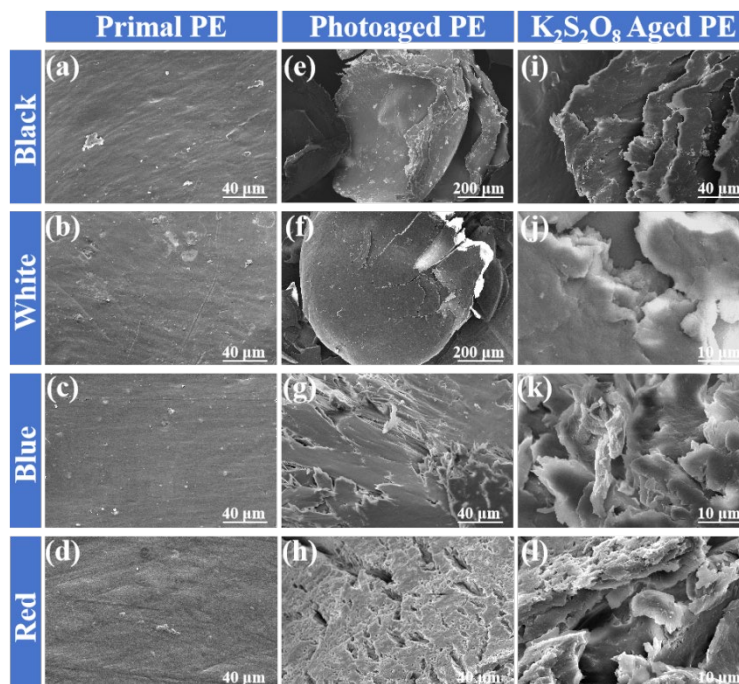


Figure 1: FESEM images of black, white, blue, and red (a-d) pristine, (e-h) photoaged, and (i-l) thermally activated $K_2S_2O_8$ aged PE.

3.1.2. Surface Functional Groups

To further investigate the changes in the physicochemical properties of MPs during the aging process, ATR-FTIR was used to analyze the changes in the surface functional groups of MPs.

Figure 2 shows the FTIR spectra of the original and aged MPs of different colors. On all spectra, several characteristic absorption peaks could be clearly observed: the absorption peaks at 2918 cm^{-1} and 2853 cm^{-1} caused by the asymmetric and symmetric stretching vibrations of $-CH_2-$, and the absorption peaks at 1467 cm^{-1} and 718 cm^{-1} caused by the bending vibration of $-CH_2-$ and the rocking vibration of C-H [16, 17]. These results confirmed that the MPs used in the experiment were PE. Compared with the original PE (Figure 2a), new peaks formed at 1711 cm^{-1} in the aged PE (Figures 2b-c), indicating the presence of C=O and suggesting that new oxygen-containing functional groups were generated on the surface of the PE samples after aging. However, the peak areas and heights of these characteristic peaks were small, possibly due to the insufficient aging time and the low amount of formed oxygen-containing functional groups.

The stretching changes of the peaks in the FTIR spectra of PE samples treated with thermal activation of $K_2S_2O_8$ (Figure 2c) were more pronounced than those in the photoaged samples (Figure 2b). After thermal activation of $K_2S_2O_8$, a new peak of C=O bond was observed in the FTIR spectrum of black PE samples (Figure 2c), while this peak was not observed in the photoaged samples (Figure 2b). This may be attributed to the light absorption characteristics of the colorants in the black PE samples. Excessive antioxidants may have been added during the production process to protect the polymer chains, thereby reducing UV-induced chain scission and requiring longer UV exposure to achieve polymer chain breakage.

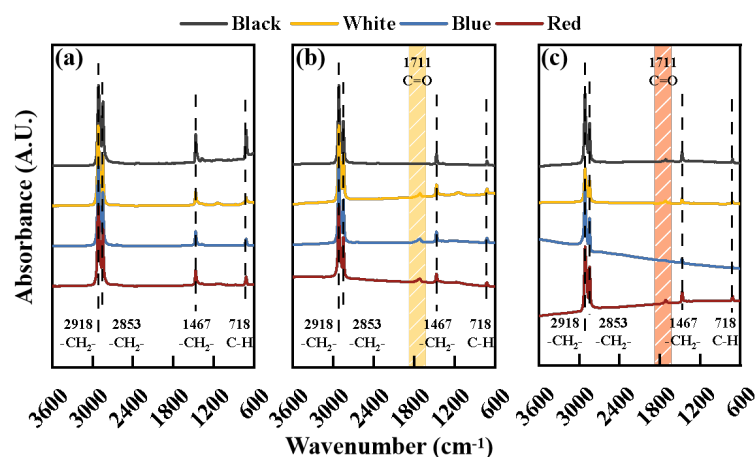


Figure 2: ATR-FTIR spectra of (a) pristine, (b) photoaged, and (c) thermally activated $K_2S_2O_8$ aged PE with different colors.

3.1.3. Carbonyl Index

The CI value is commonly used to characterize the aging degree of plastics [18]. The CI values of different colored MPs after aging are shown in **Figure 3**, with all CI values being the differences from the original state of the corresponding samples. The experimental data showed that the CI values of all aged PE samples were higher than those of the original state. Taking blue PE samples as an example, the CI value increased by 0.0369 after photoaging, and the CI value increased by 0.0631 after thermal activation of $K_2S_2O_8$ aging. The red PE samples exhibited the largest change in CI value, with an increase of 0.0765 after photoaging and an increase of 0.1081 after thermal activation of $K_2S_2O_8$ aging. The CI values of PE treated with thermal activation of $K_2S_2O_8$ were higher than those treated with photoaging, which may be due to the continuous addition of excess oxidants in the $K_2S_2O_8$ system, resulting in a large number of free radicals and continuous oxidation of PE [19]. In summary, the aging effect of the thermal activation of $K_2S_2O_8$ system was better than that of photoaging. However, no significant color changes were observed in the thermal activation of $K_2S_2O_8$ aging experiment. This may be because plastics in the environment mainly undergo photooxidation, while the aging induced by thermal activation of $K_2S_2O_8$ belongs to direct contact oxidation, which is relatively rare in the natural environment. Therefore, manufacturers may add more anti-photooxidants during production, while adding fewer or no antioxidants that slow down the direct oxidation rate.

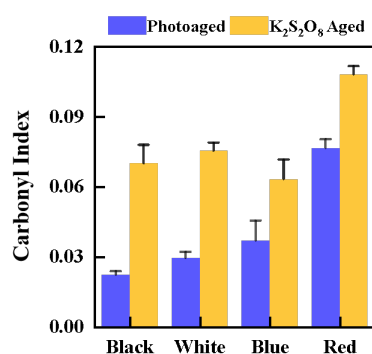


Figure 3: CI of different colored PE after photoaging and thermal activation with $K_2S_2O_8$ aging.

3.2. Adsorption Behavior of MPs for Artificial Sweeteners

Among the selected colored MPs, red PE is widely used in daily life. According to the results of the aging experiment, the aging effect of red PE was the most significant among the four colored PEs. Therefore, red PE was chosen as the adsorbent in the adsorption experiment to investigate its adsorption capacity for acesulfame.

3.2.1. Adsorption Kinetics

The results of the adsorption experiment of PE for acesulfame are shown in **Figure 4**. The entire adsorption process can be divided into three stages:

(1) 0~8 h was the initial reaction stage, during which the adsorption amount of acesulfame by PE increased rapidly, and the adsorption rate was fast. This was mainly due to the large concentration gradient between the adsorbate solution and the PE surface, which enhanced the mass transfer driving force. Additionally, the abundant empty adsorption sites on the PE surface also promoted the adsorption rate [19].

(2) The adsorption rate of acesulfame by PE decreased between 8~12 h, and the adsorption amount increased gradually, indicating that acesulfame began to occupy some of the adsorption sites on the PE surface.

(3) The adsorption rate of acesulfame by PE approached 0 between 12~24 h, and the adsorption amount reached a stable state, which was considered to have reached adsorption equilibrium. It is recommended to use the text boxes in this case.

Observing the adsorption behavior of acesulfame on the three PE, the results showed that the adsorption amount of acesulfame by aged PE was always higher than that by the original PE under the same adsorption time, and the adsorption amount of aged PE was also higher than that of the original sample at adsorption equilibrium, especially for PE treated with thermal activation of $K_2S_2O_8$. After 48 hours of adsorption, the adsorption amount of acesulfame by the original PE was 1.852 mg/g, which increased to 2.146 mg/g after photoaging, an increase of 15.9% compared with the original PE. The adsorption amount of acesulfame by PE treated with thermal activation of $K_2S_2O_8$ reached 2.478 mg/g, an increase of 33.8% compared with the original PE. The experimental results indicated that the adsorption performance of aged PE was better than that of the original PE, and PE treated with thermal activation of $K_2S_2O_8$ exhibited the strongest adsorption capacity, exceeding that of photoaged PE. This may be due to the wrinkles and cracks formed in the PE during the aging process, which increased the surface roughness of the PE and provided more adsorption sites, thereby enhancing its adsorption capacity for pollutants.

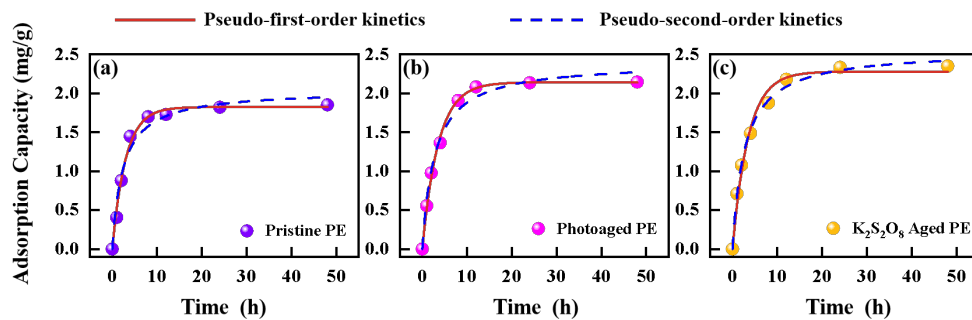


Figure 4: Adsorption kinetics fitting curves of Acesulfame on (a) pristine, (b) photoaged, and (c) thermally activated $K_2S_2O_8$ aged PE.

To study the effect of aging on the adsorption capacity of PE for acesulfame, the pseudo-first-order and pseudo-second-order kinetic models were used to analyze the adsorption behavior of PE in acesulfame solution. The adsorption kinetic model parameters are shown in **Table 1**. The results showed that for the original PE and photoaged PE, the pseudo-first-order kinetic model provided a better fit for the acesulfame adsorption data ($R^2=0.991, 0.997$) than the pseudo-second-order model ($R^2=0.968, 0.985$). Conversely, for PE treated with thermal activation of $K_2S_2O_8$, the pseudo-second-order kinetic model provided a better fit ($R^2=0.996$) than the pseudo-first-order model ($R^2=0.983$). Moreover, for the original and photoaged PE, the theoretical adsorption capacities (Q_e theoretical values of 1.825 mg/g and 2.141 mg/g) obtained from the pseudo-first-order kinetic model were closer to the experimental data (1.852 mg/g and 2.146 mg/g). For PE treated with thermal activation of $K_2S_2O_8$, the theoretical adsorption capacity (Q_e theoretical value of 2.555 mg/g) obtained from the pseudo-second-order kinetic model was closer to the experimental data (2.478 mg/g). These results indicated that the adsorption process of acesulfame by the original and photoaged PE was more in line with the pseudo-first-order kinetics, suggesting that these two adsorption processes were mainly physical adsorption between PE and acesulfame molecules. The pseudo-second-order kinetic model was more suitable for describing the adsorption process of acesulfame by PE treated with thermal activation of $K_2S_2O_8$, indicating that both physical and chemical adsorption occurred simultaneously in this adsorption process.

Table 1: Kinetic Fitting Parameters of Acesulfame on PE MPs

Sample Type	Pseudo-first-order model			Pseudo-second-order model		
	k_1	Q_e	R^2	k_2	Q_e	R^2
	(h^{-1})	(mg/g)		[$g/(mg \cdot h)$]	(mg/g)	
Pristine PE	0.334	1.825	0.991	0.205	2.047	0.968
Photoaged PE	0.279	2.141	0.997	0.150	2.403	0.985
$K_2S_2O_8$ aged PE	0.283	2.279	0.983	0.145	2.555	0.996

3.2.2. Adsorption Isotherms

The isothermal fitting curves of PE MPs for acesulfame are shown in **Figure 5**. The adsorption amount of acesulfame by MPs increased with the increase of the initial concentration of acesulfame solution, and this trend still existed in aged MPs. Moreover, at each initial concentration, the adsorption amount of aged MPs was higher than that of the original MPs.

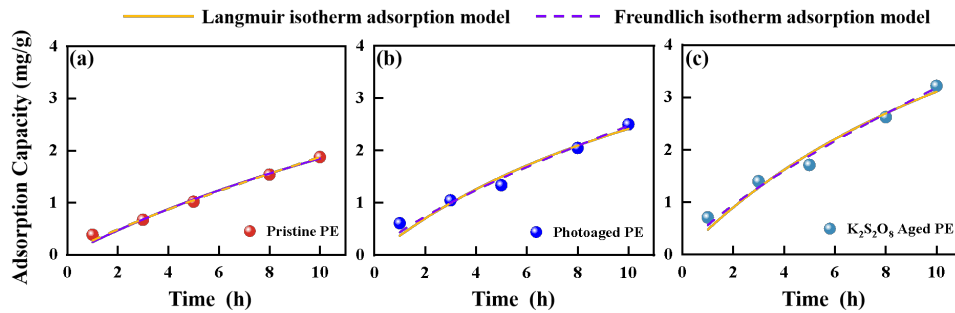


Figure 5: Isotherm adsorption fitting curves of Acesulfame on (a) pristine, (b) photoaged, and (c) thermally activated $K_2S_2O_8$ aged PE.

The adsorption data of acesulfame were fitted using the Langmuir and Freundlich models, and the fitting parameters are shown in **Table 2**. The Langmuir model assumes that the adsorption sites are energetically uniform and limited and is used to describe monolayer nonlinear adsorption behavior. The Freundlich model is one of the most commonly used nonlinear adsorption models for heterogeneous surface energy systems. The results showed that the adsorption of acesulfame by PE, whether aged or not, was more in line with the Freundlich model. The correlation coefficients R^2 of the Freundlich model fitting were between 0.978 and 0.999, which were better than those of the Langmuir model (0.945~0.979), indicating that the adsorption process between PE and acesulfame was heterogeneous [20].

Table 2: Isotherm Fitting Parameters of Acesulfame on PE MPs

Sample Type	Langmuir			Freundlich		
	K_L	Q_e	R^2	K_F	n	R^2
	(mg/L)	(mg/g)		[$(mg/g)/(L/mg)^n$]		
Pristine PE	0.035	7.077	0.979	0.271	1.191	0.999
Photoaged PE	0.063	6.217	0.945	0.438	1.331	0.997
$K_2S_2O_8$ aged PE	0.062	8.095	0.955	0.560	1.326	0.997

In the fitting analysis of the two nonlinear models, the R^2 values were all greater than 0.9, indicating that hydrophobic interactions and hydrogen bonds played a significant role in the adsorption process. The aging of MPs reduced their surface hydrophobicity, and the adsorption affinity coefficient K_F in the Freundlich model, which is related to the adsorption affinity of the adsorbent. Comparing the data in the table, it was found that $K_F, K(0.598) > K_F, G(0.438) > K_F, X(0.271)$, indicating that the affinity of acesulfame for MPs treated with thermal activation of $K_2S_2O_8$ was the highest, followed by photoaging, and the original was the lowest. This also indicated that the aging process enhanced the affinity of MPs for acesulfame. The n value in the Freundlich model fitting represents the ease of the adsorption reaction, with a larger n value indicating a more readily occurring adsorption process. In this study, the n values (1.191, 1.331, 1.393) obtained from the Freundlich model fitting were all greater than 1, and the n values of the two aging methods (1.331, 1.393) were greater than that of the original PE (0.191), indicating that the adsorption process of acesulfame on the PE surface was easy to occur, but it was easier to adsorb on the aged PE surface.

4. Conclusions

This study investigated the aging process of colored MPs and their adsorption behavior towards the environmental pollutant acesulfame. Two different aging methods, UV irradiation and $K_2S_2O_8$ treatment, were employed to simulate the aging process of MPs in the natural environment. Using characterization techniques such as FESEM and ATR-FTIR, we observed and analyzed the changes in surface morphology and the formation of functional groups of MPs before and after aging. Additionally, this study utilized adsorption kinetic and isotherm models to quantitatively analyze the adsorption characteristics of aged MPs for acesulfame, aiming to reveal the impact of the aging process on the adsorption behavior of MPs.

The main findings of this study are as follows:

The two aging methods effectively induced aging characteristics in MPs, with the thermal activation of $K_2S_2O_8$ showing a more significant effect, particularly in red MPs.

Except for black MPs, all other aged MPs generated new C=O functional groups. Among the four colored MPs, only red MPs exhibited color changes during photoaging (fading to transparency).

The aging process significantly enhanced the adsorption capacity of MPs for acesulfame. MPs treated with thermal activation of $K_2S_2O_8$ exhibited the highest adsorption amount (2.478 mg/g), followed by photoaged MPs (2.146 mg/g), while fresh MPs had the lowest adsorption amount (1.852 mg/g).

Adsorption kinetic studies indicated that the adsorption process of acesulfame by fresh and photoaged MPs was better described by the pseudo-first-order kinetic model, suggesting that adsorption under these conditions was primarily controlled by physical adsorption. In contrast, the adsorption process of acesulfame by MPs treated with thermal activation of $K_2S_2O_8$ was better described by the pseudo-second-order kinetic model, implying the involvement of both physical and chemical adsorption.

The results of the adsorption isotherm experiments showed that the adsorption behavior of all MPs conformed to the Freundlich model, indicating heterogeneous, nonlinear multilayer adsorption of acesulfame on MPs, and the adsorption process was relatively easy to occur.

Acknowledgements

The authors acknowledge the support of the National College Students' Innovation and Entrepreneurship Training Program of China. This innovation-training project, funded by the Guangxi Zhuang Autonomous Region (China), has been of great significance to our research. It is affiliated with the College of Life and Environmental Sciences at Guilin University of Electronic Technology, and the project number is S202310595288.

References

- [1] Zhao X, Wang J, Yee Leung K M, et al. Color: An important but overlooked factor for plastic photoaging and microplastic formation [J]. *Environmental Science & Technology*, 2022, 56(13): 9161-9163.
- [2] Asim N, Zulkifli A a B, Nazri N S, et al. Colours and microplastics: Bridging the gap between art, science and sustainability [J]. *Sustainable Materials and Technologies*, 2024, 42(e01152).
- [3] Horie Y, Mitsunaga K, Yamaji K, et al. Variability in microplastic color preference and intake among selected marine and freshwater fish and crustaceans [J]. *Discover Oceans*, 2024, 1(1): 5.
- [4] Li X, Huang D, Dong H, et al. Differential photoaging behaviors of different colored commercial polyethylene microplastics in water: The important role of color characteristics [J]. *Science of the Total Environment*, 2024, 956(177361).
- [5] Gao Y, Gao W, Liu Y, et al. A comprehensive review of microplastic aging: Laboratory simulations, physicochemical properties, adsorption mechanisms, and environmental impacts [J]. *Science of the Total Environment*, 2024, 957(177427).
- [6] Wang S, Gao P, Han Q, et al. Insights into photoaging behaviors and mechanisms of biodegradable and conventional microplastics in soil [J]. *Journal of Hazardous Materials*, 2024, 480(136418).
- [7] Baby M G, Gerritse J, Beltran-Sanahuja A, et al. Aging of plastics and microplastics in the environment: a review on influencing factors, quantification methods, challenges, and future perspectives [J]. *Environmental Science and Pollution Research*, 2025, 32(3): 1009-1042.
- [8] Martinho S D, Fernandes V C, Figueiredo S A, et al. Laboratory studies about microplastic aging

- and its effects on the adsorption of chlorpyrifos [J]. *Polymers*, 2023, 15(16):3468.
- [9] Wu Y, Yi R, Wang Y, et al. Light-driven degradation of microplastics: mechanisms, technologies, and future directions [J]. *Journal of Hazardous Materials Advances*, 2025:100628.
- [10] Wang X, Teo S H, Shamsuddin M R, et al. Photocatalytic degradation of organic pollutants and microplastics using Ag/TiO₂: recent advances in mechanism, synthesis and properties [J]. *Water, Air, & Soil Pollution*, 2024, 236(1): 1-25.
- [11] Li D, Xing Y, Li L, et al. Accumulation, translocation and transformation of artificial sweeteners in plants: A critical review [J]. *Environmental Pollution*, 2025, 366(125517).
- [12] Jiang L, Yu Z, Zhao Y, et al. Obesogenic potentials of environmental artificial sweeteners with disturbances on both lipid metabolism and neural responses [J]. *Science of the Total Environment*, 2024, 919(170755).
- [13] Zhao B, Rehati P, Yang Z, et al. The potential toxicity of microplastics on human health [J]. *Science of The Total Environment*, 2024, 912(168946).
- [14] LIU P, QIAN L, WANG H, et al. New insights into the aging behavior of microplastics accelerated by advanced oxidation processes [J]. *Environmental Science & Technology*, 2019, 53(7): 3579-3588.
- [15] SU J A, RUAN J H, LUO D, et al. Differential photoaging effects on colored nanoplastics in aquatic environments: physicochemical properties and aggregation kinetics [J]. *Environmental Science & Technology*, 2023, 57(41): 15656-15666.
- [16] FORMELA K, WOŁOSIAK M, KLEIN M, et al. Characterization of volatile compounds, structural, thermal and physico-mechanical properties of cross-linked polyethylene foams degraded thermo-mechanically at variable times [J]. *Polymer Degradation and Stability*, 2016, 134: 383-393.
- [17] HO T-B-C, NGUYENA T B, CHEN C-W, et al. Influence of aging processes on PE microplastics with various oxidants: Morphology, chemical structure, and adsorption behavior toward tetracycline [J]. *Environmental Technology & Innovation*, 2023, 31: 103173.
- [18] LIU P, QIAN L, WANG H, et al. New insights into the aging behavior of microplastics accelerated by advanced oxidation processes [J]. *Environmental Science & Technology*, 2019, 53(7): 3579-3588.
- [19] MO J, LIN T, ZHANG X, et al. Effects of Fe(II)-activated persulfate/sodium percarbonate (PS/SPC) pretreatment on ultrafiltration membrane fouling control and mechanisms [J]. *Desalination*, 2022, 547: 116258.
- [20] ZHANG Y, LI Y, WANG Y, et al. Adsorption of levofloxacin by ultraviolet aging microplastics [J]. *Chemosphere*, 2023, 343: 140196.